respectively. Only in the case that these energy levels are degenerated (or nearly) a σ^* structure can be expected.

Acknowledgment. This investigation has been supported by the Netherlands Foundation for Chemical Research (SON) with financial aid from the Netherlands Organization for the Advancement of Pure Research (ZWO).

Registry No. HPH_3, 25530-87-4; FPF_3, 14855-36-8; FPH_3, 56360-19-1; HPF_3, 56360-18-0; PF_5^-, 89825-40-1; PH_3, 7803-51-2; H·, 12385-13-6; $ClPH_3$, 89746-27-0; $ClPF_3$, 89746-28-1; $HPCl_3$, 89746-29-2; $FPCl_3$, 89746-30-5; $ClPCl_3$, 20762-59-8.

Electronic Structure of 1,5-Dithia-2,4,6,8-tetrazocine. Model Calculations and Spectroscopic Investigations

Rolf Gleiter,*† Richard Bartetzko,† and Dieter Cremer‡

Contribution from the Institut für Organische Chemie der Universität Heidelberg, D-6900 Heidelberg, West Germany, and the Lehrstuhl für Theoretische Chemie der Universität Köln, D-5000 Köln, West Germany. *Received September 30, 1983*

Abstract: Model calculations (ab initio and MNDO) on 1,5-dithia-2,4,6,8-tetrazocine (**2**) show that the electron-rich 10-π system prefers a planar monocyclic structure. π-Donor substituents can, however, induce a pseudo-Jahn-Teller distortion leading to a bicyclic 8-π system with a transannular S–S bond. The results of these model calculations are substantiated by investigation of the newly synthesized 3,7-di-*tert*-butyl derivative of **2** (**5**), the 3,7-diphenyl derivative (**3**), and the 3,7-bis(dimethylamino) derivative (**4**) by means of He I PE spectroscopy and linear dichroic absorption spectroscopy in the visible and near-UV region. The results obtained are best understood by assuming $b_{1u}(\pi)$ and $a_u(\pi)$ as the two highest occupied and $b_{2g}(\pi)$ and $b_{3g}(\pi)$ as the lowest unoccupied MOs of **2**.

The structure of S_4N_4 (**1a**) can be deduced by starting with a planar ring (**1b**) in which each sulfur center contributes two electrons and each nitrogen one to the π system, leading to 12 π electrons.[1,2] The degeneracy of the half-filled highest occupied e_g orbital of **1b** (D_{2h}) is removed by forming two transannular S–S bonds in **1a** (D_{2d}). If one adopts this point of view the related system of 1,5-dithia-2,4,6,8-tetrazocine (**2**) in which two opposite sulfur centers of **1** are formally replaced by carbon centers should have 10 π electrons if planar since each carbon contributes one π electron to the π system.

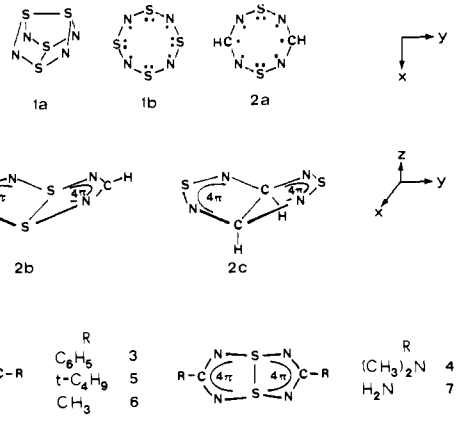

Recently derivatives of **2** have been synthesized,[3] and it has been shown by means of X-ray analysis that the 3,7-diphenyl derivative of **2** (**3**) has a planar eight-membered ring with an average S–N distance of 1.564 Å and an average C–N distance of 1.323 Å. The two phenyl groups are only slightly (9.7°) distorted out of the plane. It is interesting to note that the 3,7-bis(dimethylamino) derivative of **2** (**4**) shows a remarkable difference in its molecular shape. In contrast to the planar ring in **3**, the ring of **4** is folded along an axis through the two sulfur atoms with an interplanar angle of 101° thus giving rise to a transannular S–S distance of 2.428 Å, a value close to the transannular S–S distance found in S_4N_4 (2.58 Å). The average S–N distance (1.605 Å) as well as the average C–N distance in **4** (1.348 Å) is longer than the corresponding values found for **3**.[3]

Table I. Calculated Total Energies (hartree) and Energy Differences (kcal/mol) of **2a**, **2b**, and **2c**

basis	geometry[a]	2a	2b	2c
STO-3G	exptl	−1076.99720	−1077.06465	
		0	−42.3	
STO-3G	STO-3G	−1077.0273	−1077.06884	−1077.17102
		0	−26.0	−90.1
4-31G	exptl	−1088.08443	−1088.01958	
		0	40.7	
4-31G	STO-3G	−1088.09202	−1088.04741	−1088.02269
		0	28	43.5
STO-3G+d	exptl	−1077.53955	−1077.53750	
		0	1.3	
MNDO	MNDO	−58.24313	−58.21361	−58.16849
		0	18.5	25.3

[a] The experimental geometries **2a** and **2b** have been derived from reported data of **3** and **4**.

Both structural differences manifest themselves in the electronic absorption spectra. Compound **3** shows a long-wavelength band at 409 nm followed by a series of bands around 300 nm while **4** shows a maximum at 229 nm.

In order to understand the electronic structure of the eight-membered 1,5-dithia-2,4,6,8-tetrazocine ring, we have carried out model calculations on **2**. Furthermore, we have synthesized the 3,7-di-*tert*-butyl derivative of **2** (**5**). For **3**, **4**, and **5** we investigated the He (I) photoelectron (PE) spectra, and for **3** and **5** we recorded the electronic absorption spectra using the stretched film technique.[4]

†Universität Heidelberg.
‡Universität Köln.

(1) Gleiter, R. *J. Chem. Soc.* **1970**, 3147.
(2) Gleiter, R. *Angew. Chem.* **1981**, *93*, 442; *Angew. Chem., Int. Ed. Engl.* **1981**, *20*, 444.
(3) Ernest, I.; Holick, W.; Rihs, G.; Schomburg, D.; Shohan, G.; Wenkert, D.; Woodward, R. B. *J. Am. Chem. Soc.* **1981**, *103*, 1540.

0002-7863/84/1506-3437$01.50/0

Table II. Calculated Geometrical Parameters for **2a–c**. For a Comparison the Corresponding Experimental Data Are Listed for **3** and **4** (Bond lengths in Å, Angles in deg)

	2a		3	2b		4	2c	
parameter	STO-3G	MNDO	exptl	STO-3G	MNDO	exptl	STO-3G	MNDO
S–N	1.637	1.548	1.564	1.806	1.617	1.605	1.777	1.613
N–C	1.328	1.324	1.323	1.344	1.342	1.348	1.474	1.452
C–H	(1.08)[a]	1.110	1.08	(1.08)[a]	1.100	1.08	(1.08)[a]	1.12
S–S	4.072	3.912	3.786	2.117	2.301	2.428	2.861	4.057
C–C	3.749	3.766	3.934	3.662	3.670	3.447	1.513	1.613
NSN	122.9	123.1	127.0	103.9	107.8	101.0	96.5	103.6
SNC	137.7	141.6	141.9	108.6	118.2	118.6	109.0	111.6
NCN	141.6	133.6	129.2	134.7	121.8	124.4	62.5	111.4
HCN	109.2	113.2	115.4	112.6	119.1	117.8	119.3	109.2
SSN				95.8	90.9	89.2		
θ[b]	0	0	0	104.6	107.8	101.0	111.5	119.1

[a] Assumed bond length. [b] Dihedral angle between NCN and N'C'N'.

Table III. Calculated Net Charges of the Centers of the 1,5-Dithia-2,4,6,8-tetrazocine Ring (The First Line for Each Center Represents the MNDO Value and the Second Line the STO-3G Value)

	2a	2b	2c[c]	3[c]	4[c]	6[c]	7[c]
S	0.67[a]	0.56[b]	0.69	0.72	0.56	0.69	0.56
	0.67[c]	0.62[c]	0.35				0.61
N	−0.50[a]	−0.47[b]	−0.42	−0.53	−0.51	−0.51	−0.51
	−0.44[c]	−0.45[c]	−0.25				−0.49
C	0.21[a]	0.23[b]	0.06	0.27	0.39	0.18	0.38
	0.12[c]	0.16[c]	0.03				0.35

[a] Adopting the ring geometry of **3**. [b] Adopting the structure of the bicyclic ring of **4**. [c] Adopting the optimized structure.

Model Calculations

The main question of interest was the different S–S bond length in **3** and **4** which is reminiscent of the situation in $S_4N_5^-$ (**8**) and $S_4N_5^+$ (**9**). In **8** a relatively short transannular S–S bond length

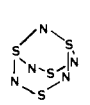

8⊖

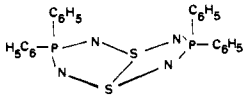

9⊕ 10

(2.73 Å)[5] is found in contrast to **9** where a transannular S–S distance of 4.01 Å has been reported.[6,7] A simple MO model starting from a planar S_4N_4 ring can rationalize these findings.[7,8] Since the bond lengths of **2** are not known, we have used MO calculations to estimate the bond lengths and angles of the planar (**2a**) and bent (**2b**, **2c**) structure of **2**. To estimate the geometry of **2a** to **2c** we used restricted HF theory employing a STO-3G basis[9] and minimizing all geometrical parameters except the C–H bond length which we assumed to be 1.08 Å. Total energies obtained at HF/STO-3G geometries have been compared to determine the relative stabilities of **2a–c**. In addition, energy calculations have been carried out for geometries of **2a** and **2b**, which were derived from the measured data of **3** and **4**, again assuming C–H bond lengths of 1.08 Å. Since the minimal basis is not suited to compare structures with different numbers of formal single and double bonds, we used the split valence 4-31G basis (44-31G for sulfur)[9] and a STO-3G basis augmented by six d functions for the heavy atoms (STO-3G+d) to compute the relative energies. In Table I we list the total energies and the energy differences obtained with the three basis sets discussed. Also, energies calculated with the MNDO[10] method are shown. All calculations except those with the STO-3G basis predict the planar conformer (**2a**) to be more stable than the bicyclic conformers **2b** and **2c**. In Table II the predicted geometry parameters for **2a–c** are listed. Those for **2a** and **2b** are compared with the parameters of the planar **3** and the bicyclic compound **4**, respectively. This comparison shows that the calculated and observed values are reasonably similar; the most pronounced difference is found for the S–N bond length. In Table III we show the calculated net charges for **2a–2c**, **3**, **4**, and **6**. It is interesting to note that according to STO-3G and MNDO calculations in the monocyclic systems (**2a**, **3**) the net charge at the sulfur centers is more positive than that in the bicyclic structures (**2b**, **4**) although a simple valence bond description suggests the opposite trend.

A population analysis for **2b** reveals that the transannular S–S bond is best described as a nearly pure $3p_\sigma$–$3p_\sigma$ bond, similar to the S–S bond in S_4N_4.[1,11] All calculations confirm that **2a** is a 10-π system, while **2b** and **2c** can be looked at as two 4-π systems delocalized over the NCN or NSN fragments, respectively. The system **2b** reminds one very much of the isovalence-electronic system $(C_6H_5)_4P_2S_2N_4$ (**10**) reported recently.[7,12]

Since in the monocyclic system, **2a**, the two highest occupied MOs ($2b_{1u}$ and $1a_u$) are essentially nonbonding π MOs (see Figure 1), the gain in energy by π delocalization is mitigated compared with a [10]annulene where only bonding π MO's are occupied.

To elucidate the energy difference between **2a** and **2b** we have correlated in Figure 1 the one-electron energies of the highest occupied MOs of **2a** with those of **2b**.

If the S–S bond is shortened we find that the $2b_{1u}$ (HOMO) is stabilized and correlates with the $7a_1$ orbital which corresponds

(4) Thulstrup, E. W.; Michl, J.; Eggers, J. *J. Phys. Chem.* **1970**, *74*, 3868. Michl, J.; Thulstrup, E. W.; Eggers, J. *Ibid.* **1970**, *74*, 3878. Thulstrup, E. W. "Aspects of Linear and Magnetic Circular Dichroism of Planar Organic Molecules"; Springer Verlag: Heidelberg, 1980; and references therein.
(5) Flues, W.; Scherer, O. J.; Weiss, J.; Wolmershäuser, G. *Angew. Chem.* **1976**, *88*, 414; *Angew. Chem., Int. Ed. Engl.* **1976**, *15*, 379.
(6) Chivers, T.; Fielding, L.; Laidlaw, W. G.; Trsic, M. *Inorg. Chem.* **1980**, *18*, 3379.
(7) Chivers, T.; Oakley, R. T. *Top. Curr. Chem.* **1982**, *102*, 117.
(8) Bartetzko, R.; Gleiter, R. *Chem. Ber.* **1980**, *113*, 1138.
(9) Hehre, W. J.; Ditchfield, R.; Stewart, R. F.; Pople, J. A. *J. Chem. Phys.* **1970**, *52*, 2769. Hehre, W. J.; Lathan, W. A. *Ibid.* **1972**, *56*, 5255. Collins, J. B.; Schleyer, P. v. R.; Binkley, J. S.; Pople, J. A. *Ibid.* **1976**, *64*, 5142.
(10) Dewar, M. J. S.; Thiel, W. *J. Am. Chem. Soc.* **1977**, *99*, 4899. Bischof, P.; Friedrich, G. *J. Comput. Chem.* **1982**, *3*, 486.
(11) Lindquist, I. *Inorg. Nucl. Chem.* **1958**, *11*, 497.
(12) Burford, N.; Chivers, T.; Codding, P. W.; Oakley, R. T. *Inorg. Chem.* **1982**, *21*, 982. Burford, N.; Chivers, T.; Richardson, J. F. *Ibid.* **1983**, *22*, 1482.

Table IV. Comparison between the First Measured Vertical Ionization Energies ($I_{V,J}$) of **5** and Calculated Orbital Energies ($-\epsilon_J$) for **2a** (All Values in eV)

band	$I_{V,J}$	assignment	$-\epsilon_J$(STO-3G, **2**)	$-\epsilon_J$(4-31G, **2**)	$-\epsilon_J$(corr[15])
1	8.39	$b_{1u}(\pi)$	7.5	9.6	8.6
2	9.2	$a_u(\pi)$	6.3	10.2	9.2
3	9.68	$b_{1g}(n)$	8.4	11.7	10.5
4		$b_{3u}(n)$	8.8	11.8	10.6
5	10.25	$b_{2u}(n)$	9.1	12.3	11.1
			11.6	14.2	12.8

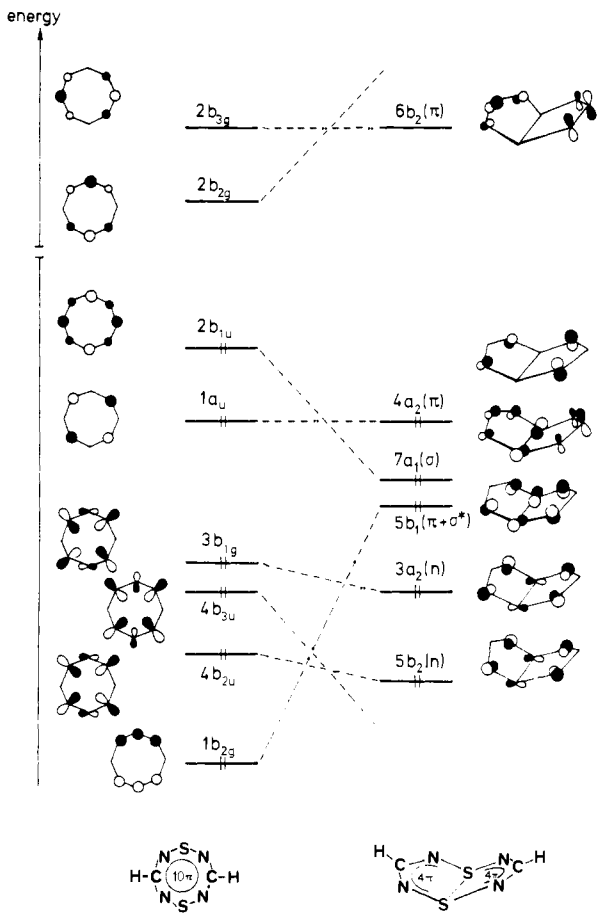

Figure 1. Qualitative correlation diagram between the six highest occupied π orbitals and the two lowest unoccupied π orbitals of **2a** with the corresponding ones in **2b**.

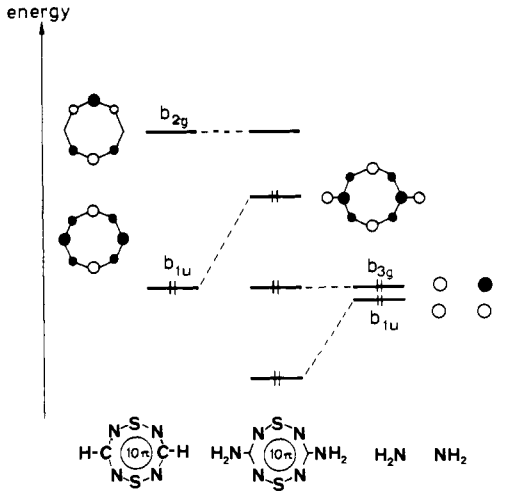

Figure 2. Qualitative interaction diagram between the HOMO and LUMO of **2a** with two 2p orbitals of NH_2 groups to yield the HOMO and LUMO of a planar 3,7-diamino-1,5-dithia-2,4,6,8-tetrazocine.

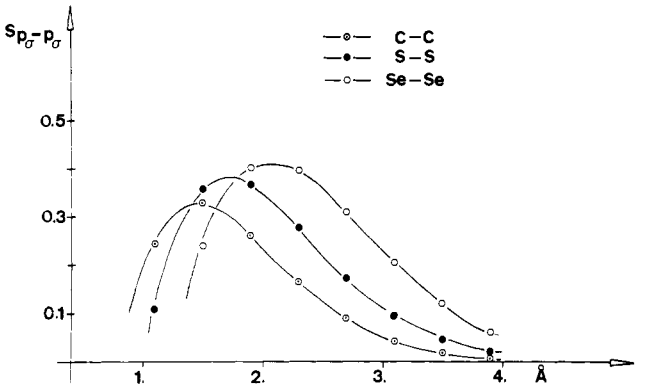

Figure 3. Overlap integrals of the type $2p_\sigma$–$2p_\sigma$ for carbon, $3p_\sigma$–$3p_\sigma$ for sulfur, and $4p_\sigma$–$4p_\sigma$ for selenium as a function of the distance. For the calculation, Slater-type orbitals were used.

to the S–S σ bond. Parallel to this stabilization we find the anticipated destabilization of the $1b_{2g}(\pi)$ orbital which is antibonding with respect to a S–S bond. The destabilization of $1b_{2g}$ and the stabilization of $2b_{1u}$ balance approximately each other. Taking into account the smaller transannular electrostatic interaction of **2a** compared with **2b** we can deduce that the stability of the planar eight-membered ring is thus the result of a delicate balance between counteracting forces. It is likely that this balance is easily perturbed, e.g., by the influence of substituents. Putting amino groups in the 3 and 7 position of **2a** will narrow the gap between HOMO and LUMO as shown in Figure 2.

This small gap may induce a pseudo-Jahn-Teller effect;[13] i.e., theory shows that there is a facile distortion along a non-totally symmetric vibrational mode which allows the mixing of HOMO and LUMO and thus enlarges the energy gap, resulting in a more stable structure. The vibrational mode that is required for the mixing of $b_{1u}(\pi)$ and $b_{2g}(\pi^*)$ is B_{3u}, belonging to the same irreducible representation as the electronic (HOMO–LUMO) transition. As we shall see later, this is indeed the case. The absorption spectra of **5** and **3** show a long wavelength band polarized perpendicular to the long axis of the molecule, consistent with the assignment of a $^1B_{3u}$ excited state. The corresponding distortion may involve a shortening of the S–S distance which leads to a stabilization of the HOMO and a destabilization of the LUMO (see Figure 1).

A similar correlation diagram as shown in Figure 1 for **2a,b** can be constructed for the correlation between **2a** and **2c**.

The observation that electron-donating substituents will cause a transannular S–S interaction as found in **4** and not a transannular C–C interaction can be rationalized on the basis of perturbation theory. At an early stage of the transannular interaction we can assume that the gain in electronic energy is overlap controlled. Due to the larger coefficients in the HOMO on S (0.55) compared with C (0.41) and the more diffuse wave functions on S compared with C the S–S interaction is more efficient than the C–C interaction. A rough measure for this is obtained by looking at the values for the $2p_\sigma$–$2p_\sigma$ overlap integral for C and for the $3p_\sigma$–$3p_\sigma$ overlap integral for S for distances between 2.5 and 4 Å (see Figure 3). This indicates that the synthesis of **2c** is only

(13) Bader, R. F. W. *Can. J. Chem.* **1962**, *40*, 1164. Bartell, L. S. *J. Chem. Educ.* **1968**, *45*, 754. Salem, L. *Chem. Phys. Lett.* **1969**, *3*, 99. Pearson, R. G. *J. Am. Chem. Soc.* **1969**, *91*, 1252, 4947.

Table V. Comparison between the Measured Vertical Ionization Energies, $I_{V,J}$, and the Calculated Orbital Energies ($-\epsilon_J$) for **3** (All Values in eV)

band	$I_{V,J}$	$-\epsilon_J$(MNDO)	$-\epsilon_J$(PPP)
		8.71 ($4b_{1u}$, π)	8.25 ($4b_{1u}$)
1	9.0	9.42 ($2a_u$, π)	9.13 ($2a_u$)
2	9.2	9.42 ($2b_{2g}$, π)	10.14 ($3b_{3g}$)
3	9.3	9.43 ($3b_{3g}$, π)	10.41 ($2b_{2g}$)
4	9.6	9.80 ($1a_u$, π)	10.4 ($1a_u$)
5	9.9	10.18 ($3b_{1u}$, π)	10.8 ($3b_{1u}$)
		10.38 ($8b_{1g}$, n)	
6	11.1		
7	12.2		

Table VI. Comparison between the Measured Vertical Ionization Energies, $I_{V,J}$, for **4** and the Calculated Orbital Energies ($-\epsilon_J$) for **7** (All Values in eV)

band	$I_{V,J}$	$-\epsilon_J$(4-31G, 7)	$-\epsilon_J$(corr[15])
		9.6 ($5a_2$, π)	8.6
1	8.15	10.2 ($9a_1$, σ)	9.2
2	8.5	10.5 ($6b_1$, π)	9.4
3	8.8	10.6 ($4a_2$, n)	9.5
		10.7 ($7b_2$, n_-)[a]	9.6
4	10.6	11.3 ($8a_1$, n_+)[a]	10.2
5	10.95	13.2 ($5b_1$, σ)	11.9
		13.3 ($6b_2$, n)	12.0

[a] Lone pairs localized mainly on the NH_2 groups of **7**.

likely to be successful if the more-stable eight-membered ring is avoided during the synthesis, i.e., if one starts with a preformed C–C bond.

The arguments just put forward suggest that the presence of electron-rich substituents in the Se analogue of **2** will cause a similar tendency for transannular Se–Se bond formation (see Figure 3).

PE Spectra of 3, 4, and 5

The PE spectra of **3**–**5** are shown in Figure 4. The first ionization potentials are listed in Tables IV to VI. As anticipated, the PE spectrum of **5** is the most simple one. It shows four peaks (bands 1–5) clearly separated from strongly overlapping bands above 11 eV. The other two spectra show a very broad band in the low-energy region which is due to the overlap of several transitions. To interpret the spectra we will rely on Koopmans' theorem, i.e., we will assume that the measured vertical ionization energies ($I_{V,J}$) can be set equal to the negative values of the calculated orbital energies ($-\epsilon_J$) ($-\epsilon_J = I_{V,J}$).[14]

We start our discussion with the PE spectrum of **5**. Using the intensity of bands as a criterion we assign the peak at 9.68 eV (bands 3 and 4) to two transitions while the first, second, and fourth peaks (bands 1, 2, and 5) are assigned to one transition. In Table IV the calculated orbital energies for the unsubstituted 1,5-dithia-2,4,6,8-tetrazocine (**2a**) are listed assuming the geometrical parameters of **3** for the eight-membered ring. Results of two basis sets (STO-3G and 4-31G) were considered. Both lead to the prediction of five MOs ($b_{1u}(\pi)$, $a_u(\pi)$, $b_{1g}(n)$, $b_{3u}(n)$, and $b_{2u}(n)$) well separated from the others. The calculations also predict that b_{1g} and b_{3u} are relatively close in energy giving rise to one unresolved band in the spectrum. If we correct the orbital energies empirically adopting Robin's approach,[15] we obtain values (column 6 of Table IV) for **2** which are reasonably close to the experimental ones for **5**, considering that the effect of the two *tert*-butyl groups has been neglected. It should be mentioned that the calculated orbital energies for **2** obtained by minimizing its geometrical parameters are close to those derived on the basis of the experimental geometry of **3**.

The PE spectrum of **3** is difficult to interpret due to the strong overlap of several transitions in the first band. In addition to the two π orbitals (b_{1u}, a_u) encountered in **5** as the two highest occupied MOs, we expect three to four additional π orbitals at relatively low energy (see Table V), namely the $2b_{2g}$, $3b_{3g}$, $1a_u$, and $3b_{1u}$ orbitals mainly localized at the phenyl rings. These orbitals are indicated below.

The sequence of the highest occupied MOs in **3** is similar to that predicted for 3,6-diphenyl-*s*-tetrazine (**11**). A comparison

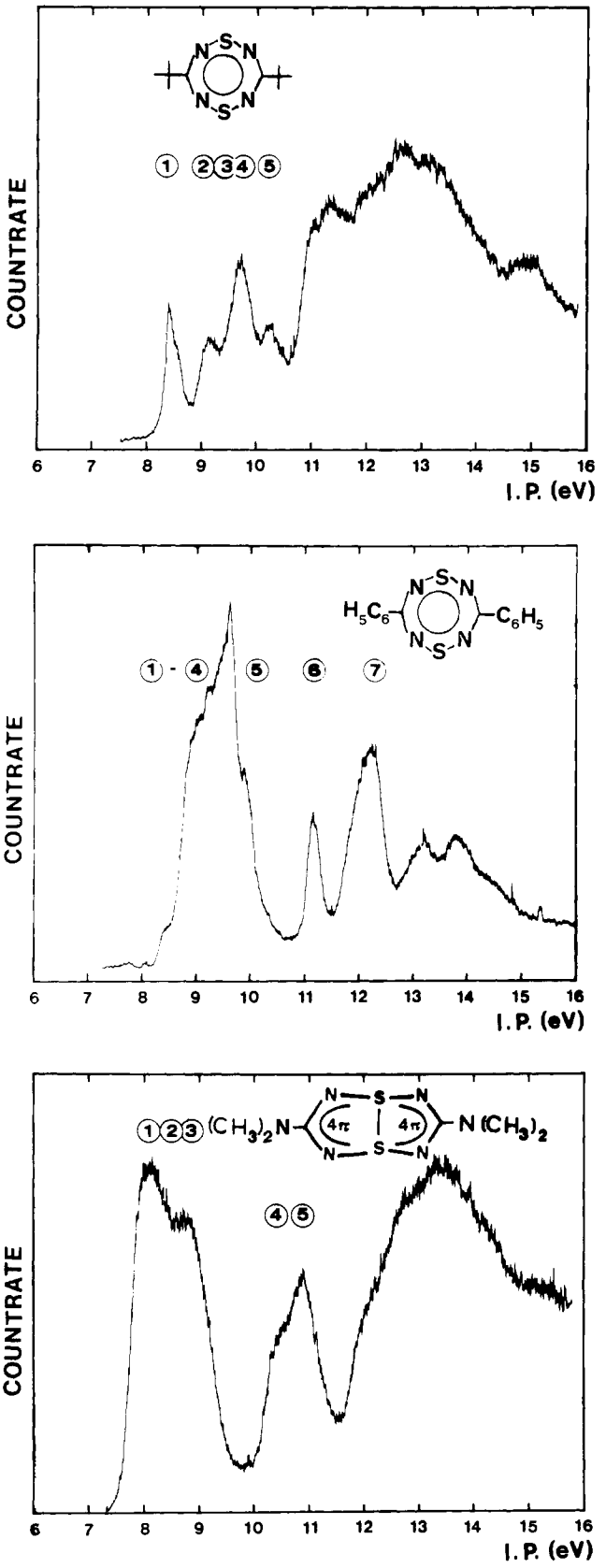

Figure 4. PE spectra of **3**, **4**, and **5**.

(14) Koopmans, T. *Physica* **1934**, *1*, 104.
(15) Brundle, C. R.; Robin, M. B.; Basch, H. *J. Chem. Phys.* **1970**, *53*, 2196.

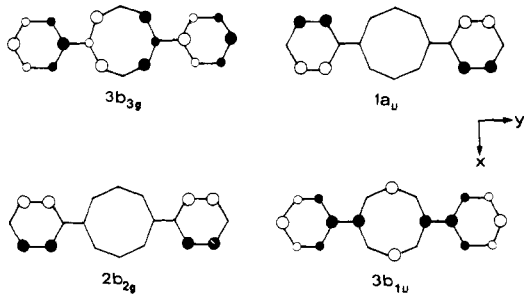

between the PE spectrum of *s*-tetrazine (**12**)[16] and that of **11**[17] shows four additional π levels in the region below 11 eV due to the two phenyl rings. In Table V we list the results of MNDO[10] and PPP[18] calculations which predict six π levels below 11 eV. Due to the strong overlap of the bands any assignment has to be tentative. Therefore no assignment has been made in Table V.

A similar situation is encountered with the PE spectrum of **4**. We observe two broad peaks (bands 1–3 and 4, 5) below 12 eV. Unfortunately there are no spectra of similar compounds available to help in assigning the bands empirically and thus we have to rely on calculations. In Table VI we have listed the results of a model calculation on **7** as well as the corrected ionization potentials according to Robin.[15] The comparison between measurement and calculation suggests the assignment of five to six transitions for bands 1–3. Further research is necessary for a definitive assignment.

The comparison between the PE spectra of **5** and **4** confirms the qualitative correlation diagram given in Figure 1 in so far as the first five transitions are much closer together in the PE spectrum of **4** (~0.7 eV) than in the spectrum of **5** (~1.8 eV).

Polarized Absorption Spectra

In Figure 5 we show the absorption spectra of **3** and **5** in stretched polyethylene at room temperature indicating absorption polarized along the long (y) axis of the molecule and the short (x) axis of the molecule. The spectra shown are those obtained after the reduction and the corrections for the basis line.

The absorption spectrum of **5** shows four bands between 25 000 and 47 000 cm^{-1}. Two of them, bands A and D, are intense while band B and C are found to be relatively weak. Using the stretched film technique we find that band A of **5** is polarized perpendicular to the long axis while band D is found to be polarized parallel to the long axis of **5**. Between these two intense bands we find a region of mixed polarization between 35 000 and 37 000 cm^{-1}.

The polarized absorption spectrum of **3** shows a weak band (A) with vibrational fine structure at 24 000 cm^{-1}. Between 30 000 and 40 000 cm^{-1} our stretched film measurements reveal a very broad peak polarized parallel and one polarized perpendicular to the long axis of the molecule. The vibrational fine structure and shape of the long axis polarized band indicate the presence of at least two transitions (labeled B and C). A broad perpendicular band (D) is found nearly at the same energy as band C. Between 40 000 and 45 000 cm^{-1} we find bands polarized parallel to the long axis (E) and perpendicular to it (F).

Comparison with Theory

In Table VII we have listed results obtained by the PPP–CI model treating the π system of **3** and **5** only. Using the standard parameters referred to later we predict for **5** three allowed transitions between 25 000 and 45 000 cm^{-1}. The first one at 27 100 cm^{-1} is polarized perpendicular to the long axis and corresponds to the LUMO ← HOMO transition with the B_{3u} symmetry referred to previously. According to these calculations band B and D are assigned to the transitions $2b_{1g}$(LUMO) ← $1a_u$ and $2b_{2g}$ ← $2b_{3u}$(HOMO). The calculations reproduce the energy, relative intensity, and polarization direction quite well.

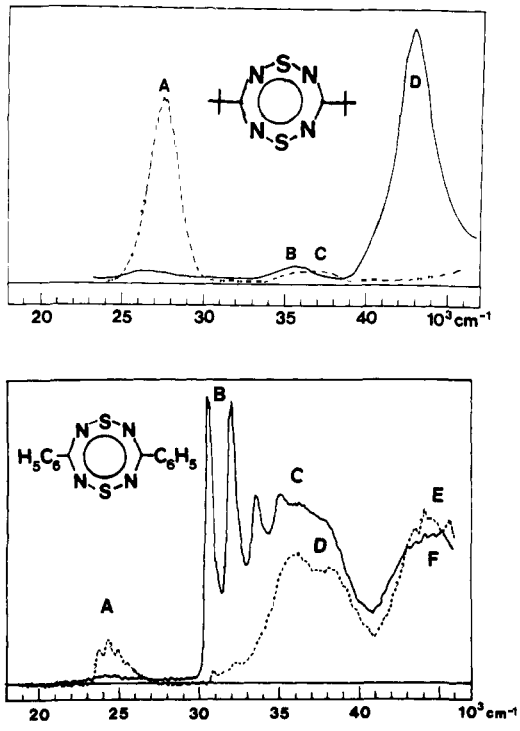

Figure 5. Absorption spectra of **3** and **5** in stretched polyethylene. The figure shows the reduced absorption curves corresponding to y polarization (full line) and x or z polarization (broken line).

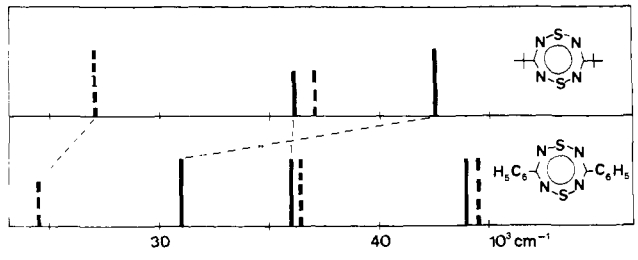

Figure 6. Correlation between the first absorption bands of **3** and **5**. The polarization direction of the bands is indicated by full lines (parallel to the long axis) and broken lines (perpendicular to the long axis of the molecules).

Band C is not reproduced by the PPP–CI model. We assign it tentatively to a π^* ← n transition. In line with this is its low intensity, the polarization direction, and the fact that there are several high-lying n orbitals found in **5** (see PE results). An allowed transition polarized perpendicular to the molecular plane ($2b_{2g}(\pi^*)$ ← $b_{3u}(n)$) is suggestive.

For **3** the PPP–CI model reproduces the recorded six bands quite well concerning their energies, relative intensities, and polarization directions. The first band corresponds to a transition of B_{3u} symmetry and is mainly localized in the eight-membered ring. Band B of the electronic absorption spectrum of **3** is only partly localized in the heteroring system and may be correlated with band D of the spectrum of **5** (see Figure 6). The strong long wavelength shift of this band can be explained by strong stabilization of $4b_{3g}(\pi^*)$ by the two phenyl rings. Band C of the spectrum of **3** is correlated in Figure 6 with band B of **5**. The relatively small shift of this band (Figure 6) is understandable since $2a_u$ and $3b_{2g}$ of **3** (and $2b_{2g}$ and $1a_u$ of **5**) both have nodes at the carbon centers and thus the influence of any substituents is anticipated to be small.

Concluding Remarks

The model calculations on **2a** and **2b** show that there is a delicate balance in energy between the electron-rich delocalized 10-π monocyclic system and the partly localized bicyclic system. Electron-rich substituents tend to favor the latter system. This

(16) Gleiter, R.; Heilbronner, E.; Hornung, V. *Helv. Chim. Acta* **1972**, *55*, 255.
(17) Thulstrup, E. W.; Spanget-Larsen, J.; Gleiter, R. *Mol. Phys.* **1979**, *37*, 1381.
(18) Pariser, R.; Parr, R. G. *J. Chem. Phys.* **1953**, *21*, 446. Pople, J. A. *Trans. Faraday Soc.* **1953**, *49*, 1375.

Table VII. Observed and Calculated Transitions for **3** and **5**[a]

	observed				calculated				
compd	band	$\tilde{\nu}_{max}$	log	p	$\tilde{\nu}$	f	p	symmetry	leading configurations (%)
5	A	27.4	4.1	⊥	27.1	0.30	⊥	$^1B_{3u}$	$2b_{2g} \leftarrow 2b_{1u}$ (85)
	B	35.7		∥	32.9	0.14	∥	$^1B_{2u}$	$2b_{2g} \leftarrow 1a_u$ (72), $2b_{3g} \leftarrow 2b_{1u}$ (25)
			3.3						
	C	36.6		⊥					
	D	42.7	4.3	∥	41.5	1.76	∥	$^1B_{2u}$	$2b_{3g} \leftarrow 2b_{1u}$ (72), $2b_{2g} \leftarrow 1a_u$ (25)
		23.4							
3	A	24.0	3.9	⊥	25.9	0.21	⊥	$^1B_{3u}$	$3b_{2g} \leftarrow 4b_{1u}$ (77), $4b_{3g} \leftarrow 2a_u$ (18)
		24.5							
		31.1							
	B	32.5	4.5	∥	28.7	0.67	∥	$^1B_{2u}$	$4b_{3g} \leftarrow 4b_{1u}$ (85)
		33.9							
	C	36.0		∥	35.1	1.90	∥	^1B_u	$3b_{2g} \leftarrow 2a_u$ (81), $4b_{3g} \leftarrow 4b_{1u}$ (10)
			4.4						
	D	36.0		⊥	39.1	0.41	⊥	$^1B_{3u}$	$4b_{3g} \leftarrow 2a_u$ (77), $3b_{2g} \leftarrow 4b_{1u}$ (18)
	E	43.5		⊥	43.0	0.28	⊥	$^1B_{3u}$	$4b_{2g} \leftarrow 4b_{1u}$ (48), $4b_{3g} \leftarrow 1a_u$ (20)
			4.4						
	F	44.0		∥	45.7	0.01	∥	$^1B_{2u}$	$4b_{2g} \leftarrow 2a_u$ (99)

[a] The table indicates wave numbers $\tilde{\nu}$ in units of 1000 cm^{-1}, log ϵ values in cyclohexane, and observed polarization directions p. Symmetries are given in the point group D_{2h}. For **5** the model calculations refer to the dimethyl compound.

situation is similar to that encountered in the case of the isovalent electronic system $S_4N_4^{2+}$, for which two different structures (a planar and a nearly planar one) have been reported.[19] The structural details like bond angles and bond lengths seem to depend on a demand for maximum delocalization as well as on the anion and the neighbors in the solid state.

With respect to the 10-π systems just discussed a molecule like **13** deserves some interest. Here the electron-rich substituents might favor a planar structure. Furthermore, electron-withdrawing substituents on the phenyl rings of **10** should also be of interest in view of a planar system.

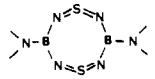

13

Our investigations of the PE and electronic spectra allow us also to deduce the sequence of the lowest unoccupied orbitals of the 10-π systems. Our data are best rationalized if we assume $2b_{2g}$ for the LUMO and $2b_{3g}$ for the one next to it.

Experimental Section

The He I PE spectra were recorded on a PS 18 spectrometer (Perkin-Elmer Ltd., Beaconsfield, England). The calibration was done with Xe and Ar. A resolution of 20 meV was achieved with the $^2P_{3/2}$ Ar line. The samples had to be heated to the following temperatures: 120 °C (**3**), 108 °C (**4**), and 70 °C (**5**).

The linear dichroic absorption spectra were obtained in a stretched polyethylene sheet at room temperature on a Cary 17 instrument. The sheet was dipped in a chloroform solution of the compound to be investigated, stretched 500%, and after evaporation of the solvent, rinsed with ethanol. The absorption curves were recorded in digital form which was used for the production of the reduced spectra.[4]

3,7-Diphenyl-1,5-dithia-2,4,6,8-tetrazocine (**3**) and the bis(dimethylamino) derivative (**4**) were supplied by Dr. I. Ernest, CIBA-GEIGY Ltd., Basel.

3,7-Di-*tert*-butyl-1,5-dithia-2,4,6,8-tetrazocine (5). The synthesis of **5** was carried out analogously to that of **3** reported in the literature.[3] To a solution of 2.2 g (16 mmol) of pivaloylamidine hydrochloride[20] and 9.52 mL (64 mmol) of diazabicycloundecene in 20 mL of absolute CH_2Cl_2 a solution of 1.52 mL (24 mmol) of freshly distilled sulfur dichloride in 10 mL of absolute CH_2Cl_2 was added dropwise over 15 min with stirring under nitrogen in an ice water bath. After 1 h, the ice water bath was removed and the mixture was stirred for an additional 3 h at room temperature. The dark red solution was diluted with CH_2Cl_2 and washed three times with water (3 × 100 mL) and with saturated NaCl solution (1 × 100 mL). Drying the organic phase over Na_2SO_4 and evaporating under vacuum afforded 1.7 g of red-brown oil. After the oil was washed with pentane (7 × 50 mL) and the residual solvents were evaporated a yellow powder remained: 300 mg (1.1 m mmol, 13.7%); mp 108–109 °C. Anal. Calcd. for $C_{10}H_{18}N_4S_2$ (258): C, 46.51; H, 6.97; N, 21.70; S, 24.80. Found: C, 46.74; H, 7.01; N, 21.31; S 24.70. UV λ_{max} (MeOH) 363 (ϵ 9775), 277 (2035), 243 (16020), 220 (6380); IR (KBr) $\tilde{\nu}$ 2900, 1650, 1480, 1400, 1360, 1250, 1130, 820 cm^{-1}; ^1H NMR (60 MHz in $CDCl_3$) δ 1.55 (s); ^{13}C NMR (75.46 MHz in $CDCl_3$) δ 1.7, 30.1, 144.8.

Calculations. For the PPP calculations on **3** and **5** we used the experimental geometry of **3**.[3] The parameters used were the following: U_C = −11.42 eV, U_S = −20.0 eV, U_N = −14.1 eV, $\gamma_{CC} = \gamma_{SS}$ = 10.84 eV, γ_{NN} = 12.30 eV, and $\beta_{CN} = \beta_{SN}$ = −2.31 eV. The two center integrals were calculated according to the Mataga–Nishimoto approximation.[21]

Acknowledgment. We are grateful to the Deutsche Forschungsgemeinschaft, the Fonds der Chemischen Industrie, and the BASF Aktiengesellschaft for financial support. Ab initio calculations have been carried out at the Regionales Rechenzentrum Köln utilizing a CDC CYBER 76. We thank Dr. J. Spanget-Larsen for recording the LD spectrum of **5**. We are very grateful to Dr. I. Ernest for a gift of **3** and **4** and his comments.

Note Added in Proof. When this paper was in print a supplementary ESCA investigation on **3** and **4** appeared.[22]

Registry No. 2a, 77536-71-1; **2b**, 89909-09-1; **2c**, 89909-10-4; **3**, 76843-75-9; **4**, 89909-07-0; **5**, 89909-08-0.

(19) Gillespie, R. J.; Slim, D. R.; Tyrer, J. D. *J. Chem. Soc., Chem. Commun.* **1977**, 153. Gillespie, R. J.; Kent, J. P.; Sawyer, J. F.; Slim, D. R.; Tyrer, J. D. *Inorg. Chem.* **1981**, *20*, 3799.

(20) "Organic Synthesis"; Wiley: New York, 1956; Collect. Vol. I, p 5.

(21) Mataga, N.; Nishimoto, K. *Z. Phys. Chem.* **1957**, *13*, 140.

(22) Boutique, J. P.; Riga, J.; Verbist, J. J.; Delhalle, J.; Fripiat, J. G.; Haddon, R. C.; Kaplan, M. L. *J. Am. Chem. Soc.* **1984**, *106*, 312.